Journal of Coastal Research	24	2	489–499	West Palm Beach, Florida	March 2008

Comparison of the CEST and SLOSH Models for Storm Surge Flooding

Keqi Zhang†‡, Chengyou Xiao†, and Jian Shen§

†International Hurricane Research Center
Florida International University
Miami, FL 33199, U.S.A.

‡Department of Environmental Studies
Florida International University
Miami, FL 33199, U.S.A.

§Virginia Institute of Marine Science
College of William and Mary
Gloucester Point, VA 23062, U.S.A.

ABSTRACT

ZHANG, K.; XIAO, C., and SHEN, J., 2008. Comparison of the CEST and SLOSH models for storm surge flooding. *Journal of Coastal Research,* 24(2), 489–499. West Palm Beach (Florida), ISSN 0749-0208.

The Coastal and Estuarine Storm Tide (CEST) model for the boundary-fitted curvilinear grid has been developed recently to simulate a hurricane-induced storm surge. A new wetting-drying algorithm was based on accumulated volume and was created for simulating overland flooding. To evaluate the capability of the CEST model, it was compared with the well-established storm surge model—Sea, Lake, and Overland Surge from Hurricane (SLOSH)—in model grid representation and surge inundation prediction. Two models were compared: first, by carrying out storm surge simulations for Hurricanes Andrew (1992), Hugo (1989), and Camille (1969) over SLOSH's coarse polar grids with cell sizes of 500–7000 m. Results show that the CEST model agreed better with field observations of storm surge flooding. The CEST model was further evaluated by applying it to a fine-resolution curvilinear grid, which has cell sizes of 100–200 m at the hurricane landfall area, along with a superior representation of coastal topography. Comparison of the model results with field-measured elevations of high water marks and the locations of debris lines indicated that the CEST model, with the use of a fine-resolution grid, greatly reduced the uncertainty in computing storm surge flooding.

ADDITIONAL INDEX WORDS: *Hurricane, storm surge, storm tide, SLOSH, CEST.*

INTRODUCTION

The greatest hazard to human life posed by hurricanes is drowning in a storm surge. Historically, storm surges have accounted for more than 90% of fatalities resulting from hurricanes. Salt water flooding is also a major cause of damage to coastal property and infrastructure. To avoid loss of life during such flooding events, the Sea, Lake, and Overland Surge from Hurricane (SLOSH) model was developed by the National Weather Service (NWS) of the National Oceanic and Atmospheric Administration (NOAA) several decades ago to delineate evacuation zones. The death toll in the United States from storm surge flooding has declined drastically over the last several decades because of the execution of proper evacuation policy. Despite its success, the SLOSH model suffers several drawbacks, such as neglect of tide and insufficient spatial resolution for computing overland flooding.

Recently, a three-dimensional (3D) Coastal and Estuarine Storm Tide (CEST) model for a curvilinear grid has been developed to simulate coastal and estuarine hydrodynamic processes (Xiao, Zhang, and Shen, 2006). This model solves the full momentum equation together with the continuity equation while maintaining nonlinear advection and diffusion terms. The model is driven by atmospheric pressure, surface wind, and tide and is capable of simulating the storm tide, which includes both storm surge and tide. The model simulates overland flooding of storm surges with a new and robust wetting-drying algorithm. The purpose of this study is to evaluate the performance of the CEST model by comparing simulations with those from SLOSH and with field observations. SLOSH was selected as a benchmark model for the evaluation because it is the only model in the United States that has been verified extensively against field observations for overland flooding along the East and Gulf coasts.

SLOSH AND CEST MODELS

A brief review of the SLOSH and CEST models is presented in this section. The review focuses on the model capability for storm surge and inundation simulations. Detailed descriptions about two models can be found in Jelesnianski, Chen, and Shaffer (1992) and Xiao, Zhang, and Shen (2006).

SLOSH

The SLOSH model was developed by the NWS in the early 1980s. The model was designed in such a way that the surge forecast could be conducted with minimal local calibration (Jelesnianski, Chen, and Shaffer, 1992). For the model to cover a large area and maintain high resolution near the coast without losing computation efficiency, a polar grid system with gradually varying cell sizes was chosen to represent the model domain. This allows the model mesh to cover a basin extending from the inland area possibly flooded by storm surge to deep water about 150–200 km offshore. How-

DOI: 10.2112/06-0709.1 received 25 May 2006; accepted in revision 29 September 2006.

This study was partially sponsored by the Florida Hurricane Research Alliance Program.

ever, some basins are not large enough to calculate surge propagation from the open ocean to the coast. To account for the effect of surge propagation, the SLOSH model usually initializes the water level at the boundaries by averaging records of nearby tide gauges for approximately 2 days before storm arrival. The model was tested and verified for many hurricanes that have well-documented parameters and surge observations. Comparison between computed values and field observations from 13 landfall hurricanes along the U.S. East and Gulf coasts indicates that the error of computed maximum surge heights is about ±20%.

SLOSH is a two-dimensional (2D) model but is not simply a depth-averaged model. The bottom stress is not determined by the depth-averaged velocity; instead, it is based on a vertical velocity profile considering the effect of Ekman drift (JELESNIANSKI, 1970; KIM and CHEN, 1999). SLOSH incorporates finite amplitude effects but excludes advective and baroclinic terms in the equations of motion. The model is forced by surface stress and atmospheric pressure and does not simulate tide. The model can reproduce the time history of a storm surge, and the predicted surges are comparable to water level records after astronomical tides are removed.

Great effort was made to deal with the inundation processes of storm surges over natural or human-modified topographic features along the coast. A dedicated computation scheme was developed for SLOSH with a B grid to simulate wetting and drying processes. Both natural and man-made linear or small features with high elevations, such as coastal ridges, barrier islands, and levees, were represented by "barriers." A barrier is a thin "wall" along the cell boundaries with a user-specified elevation. A 2D flow will exist at a node if at least one of the four surrounding grid cells are wetted, and the water surface elevation at the node is greater than the highest water surface of four surrounding grid cells (JELESNIANSKI, CHEN, and SHAFFER, 1992). In the initial flooding of a grid cell, the flow is driven only by gravity forces, and the surface driving forces are ignored. To accommodate the flow passing through narrow channels with widths less than the cell size (*e.g.,* inlets and small rivers), the model allows users to specify channel width in terms of the portion of the cell size and use a one-dimensional (1D) model to simulate the flow. In this way, the water exchange between large grid cells and narrow inland channels is handled properly.

CEST

The Coastal and Estuarine Storm Tide (CEST) model is a 3D, finite difference model developed by the International Hurricane Research Center (Florida International University, Miami, Florida) to simulate estuarine and coastal flooding induced by hurricanes (XIAO, ZHANG, and SHEN, 2006). The CEST model is forced by winds, atmospheric pressures, and astronomical tides or a time series of water levels at open boundaries. It is capable of simulating storm tides as well as the wind-driven circulation at estuaries and coasts. The model can also include river flow in the simulation.

The CEST model extends the POM/ECOM model (BLUMBERG and MELLOR, 1987) to a nonorthogonal curvilinear grid to better fit the major coastal topographic features, such as barrier islands. Using the velocity contravariant component technique, we transform the POM/ECOM model equations to the coordinates of a horizontal generalized curvilinear grid. To improve the computation efficiency and stability of the model, a semi-implicit scheme (CASULLI and CHEN, 1992) is employed to produce a discrete form of the control equations. The water level gradient, bottom friction, and vertical viscosity terms that affect numerical stability are treated implicitly, and the remaining terms are treated explicitly. Because each momentum equation contains water elevation gradient terms from both directions, introduced by coordinate transformation, we treat one direction of the gradient (main direction) implicitly and the other direction of the gradient explicitly. This ensures that the linear equations are both symmetric and positive definite; thus, a preconditioned conjugate gradient method can be used to solve the equations.

The model can also run over the orthogonal, conformal grid, such as the polar grids used by SLOSH, without modification of the numerical algorithms. With varying cell sizes, the curvilinear grid can generate fine cells at the coast and coarse ones at open ocean to improve simulation of storm surge overland flooding.

A novel, mass-balanced algorithm that is based on accumulated water volume was developed for the C grid–based CEST model to simulate wetting-drying processes. The water levels and elevations at both a cell center and its four boundaries are involved in calculating the accumulated water volume. During flooding, if the water level elevation at the center of a wet cell is higher than that at the dry cell more landward, and the water depth at the shared boundary between these two cells is greater than a predefined threshold, the water is allowed to flow from the wet cell into the dry cell and accumulate there. The water interchange velocities (u_k) cross four shared boundaries between a dry cell, and its wet neighbors are obtained by solving a simplified 1D momentum equation

$$\frac{\partial u_k}{\partial t} + g\frac{\partial \zeta_k}{\partial x_k} + \frac{C_d}{H}|u_k|u_k = 0 \quad (1)$$

where C_d is the bottom friction coefficient and is set to 2.6 × 10^3 (SHI, SUN, and WEI, 1997), x_k is the direction of u_k, ζ_k is the free surface elevation, and H is the water depth. For time step, n, the accumulated water volume is calculated by

$$\Delta Q_{i,j}^{n} = \Delta Q_{i,j}^{n-1} + \sum_{k} (\Delta t \times u_k^n \times A_k^n) \quad (2)$$

where $\Delta Q_{i,j}^{n-1}$ is the accumulated water volume in the dry cell from the previous time step, and Σ represents the sum of water volumes flowing into the cell through the boundaries. A_k^n is the cross-sectional area at the kth shared boundary between a wet and dry cell. Once the water depth estimated from the accumulated water volume in the dry cell is greater than a given threshold, the dry cell becomes wet and is included in the grid for further computation. Similar to SLOSH, the effect of linear features with high elevation such as levees can be introduced into the model by setting barriers along the cell boundaries.

During receding water, a boundary cell is set to be dry if the water depth at the cell center is less than a predefined

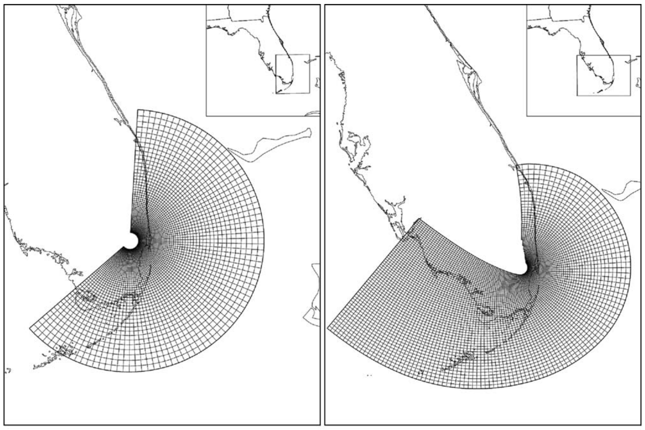

(a) (b)

Figure 1. Coarse-resolution polar grid for the SLOSH model (a) and a fine-resolution curvilinear grid for the CEST model (b) at the South Florida coast. The grid resolution for the CEST model is reduced for display purposes, and the actual grid resolution is four times higher.

threshold value. No water exchange occurs across the four boundaries of this dry cell. Note that the water could stop flowing across a cell boundary if the water depth at this boundary is less than the threshold, even before the cell is completely dry. In such a case, if the water depths at four boundaries of a cell are all less than the threshold, the cell is set to be dry.

Model Domain

One way to evaluate the performance of the CEST model is to examine whether the model can reproduce simulations similar to those from SLOSH under the same input and boundary conditions. The SLOSH model employs a coarse polar grid and subgrid barriers to delineate the coastal topographic and bathymetric features. To examine the effect resulting from the differences in wetting-drying algorithms and in nonlinear momentum equations, a 2D CEST model was applied to the SLOSH polar grids to simulate storm surges from Hurricanes Andrew, Hugo, and Camille. Subgrid feature barriers from the SLOSH model are included in the CEST simulation, but 1D channel flow is not included because of the difference in model algorithms.

Figure 1a shows the coarse model grid for SLOSH along the south Florida coast, which covers a radius of 180 km from Miami and includes all low-lying lands in the vicinity of Biscayne Bay. The grid cell sizes in Biscayne Bay range from 700 to 1000 m. The elevations for the grid cells come from U.S. Geological Survey (USGS) topographic maps and ground surveys. Special features such as coastal ridges, levees, and canals were incorporated into the model as subgrid features.

It is also necessary to examine the possible advances of the CEST model in storm surge prediction on the basis of improved algorithms and increased grid resolutions. Therefore, the second step in evaluating the CEST model is to examine model performance over a fine-resolution curvilinear grid. Figure 1b shows the fine-resolution curvilinear grid used by

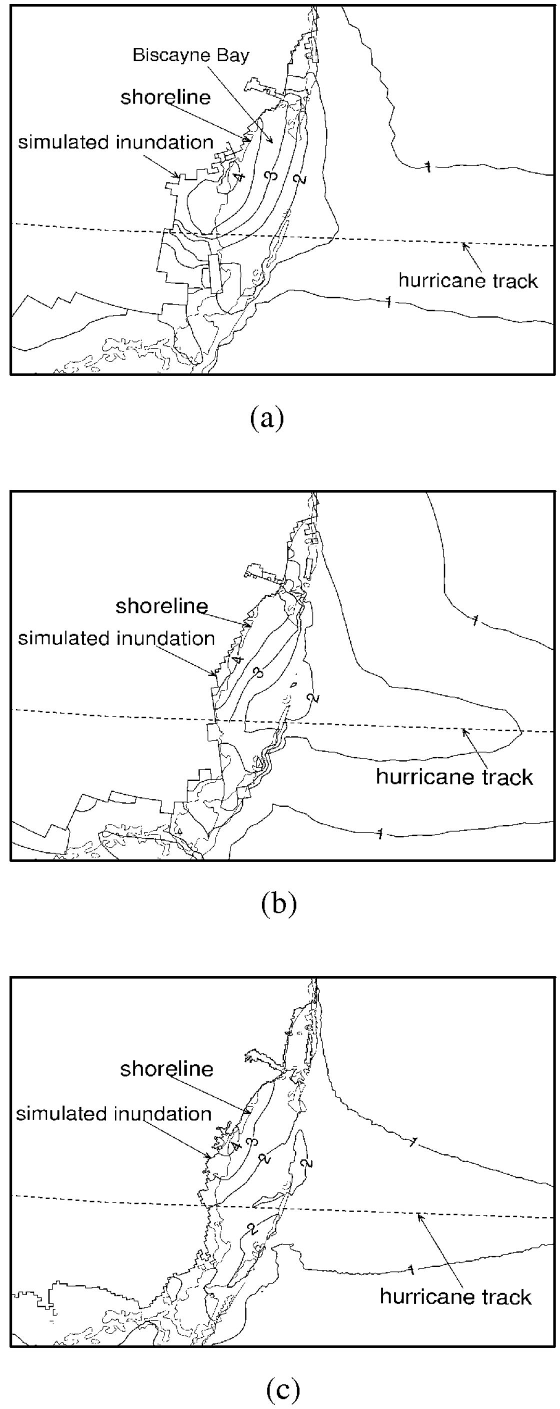

Figure 2. Contours of computed maximum storm surges and inundation lines from SLOSH (a), CEST with the coarse-resolution grid (b), and CEST with the fine-resolution grid (c) for Hurricane Andrew at the South Florida coast. The shoreline is represented by a dashed line.

the CEST model for Hurricane Andrew. The grid includes both the east and west parts of Florida and covers a larger domain than the SLOSH basin. In addition, instead of following a straight line, the inland boundary of the grid fits curved linear features with high elevations such as coastal ridges so their effect on blocking storm surges can be simulated better. The grid resolution is about 100–200 m around the landfall area.

The USGS 10-m digital elevation model (DEM) data were used to derive the elevation over the fine-resolution model grid if the data were available for the study area, and the 30-m DEM data were used for areas without 10-m DEMs. The NOAA 2-minute Global Relief Model (ETOPO2) and 3-arc-second Coastal Relief Model were combined to obtain bathymetric data for the model grid. No subgrid features from SLOSH basins were introduced into the CEST model domain because major subgrid features such as barrier islands can be directly delineated by the fine-resolution grid.

Boundary Conditions

The inverse pressure-adjusted boundary conditions were used as the open boundary conditions for both SLOSH and CEST over coarse grids. No tide was forced on the open boundaries because the SLOSH model does not include the tide component. Both CEST and SLOSH models allow the outgoing wave to propagate out of the model domain with the use of a radiation boundary condition.

The CEST model for a high-resolution curvilinear grid was forced by nine tidal constituents, including M_2, S_2, K_1, O_1, Q_1, K_2, N_2, M_4, and M_6 at its open boundaries. The forcing harmonic constants were obtained from the U.S. Army Corps of Engineers' (USACE) East Coast 2001 database of tidal constituents (Mukai *et al.,* 2002). The inverse pressure adjustment was also superimposed on the tidal force. Other boundary conditions were the same as those used for the coarse-grid model simulation.

Wind Field Modeling

The accuracy of storm surge prediction depends largely on the wind field prescribed to the model because storm surge intensity is highly sensitive to wind forcing. The wind field is usually estimated by either analytical parameter methods or numerical models. For example, a common practice for storm surge simulation is to construct the wind field by fitting Holland's analytical cyclone model (Holland, 1980; Hubbert and McInnes, 1999; Tang and Grimshaw, 1995). A Planetary Boundary Layer hurricane model has been developed by the USACE Waterways Experimental Station (Scheffner and Fitzpatrick, 1997) to predict the surface wind field in terms of the predicted storm path. Recently, surface wind observations analyzed by the Hurricane Research Division (HRD) of NOAA were available for driving a storm surge model. The HRD wind field is created on the basis of all available surface wind observations from buoys, coastal and marine automated observation platforms, ships, and other facilities and provides a more realistic wind input for simulating storm surges of past events (Houston *et al.,* 1999; Powell *et al.,* 1998).

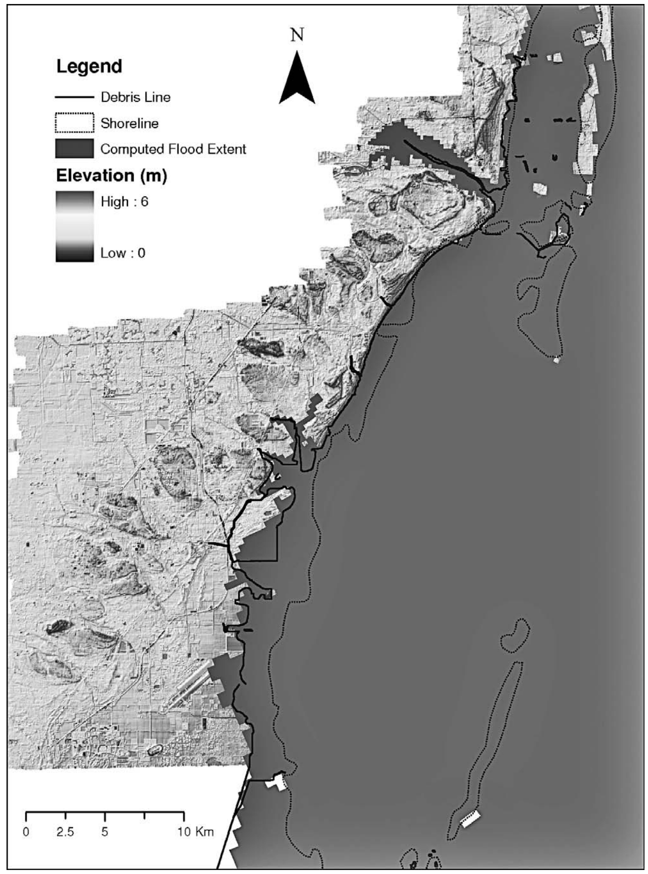

Figure 3. Comparison of simulated inundation for Hurricane Andrew by the fine-resolution CEST model with field observations. The Atlantic Coastal Ridge blocked further flooding from the surge of Hurricane Andrew along the northern mainland coastline of Biscayne Bay. The elevation data refer to the NAVD 1988 vertical datum. **For a color version of this figure, see page 447**.

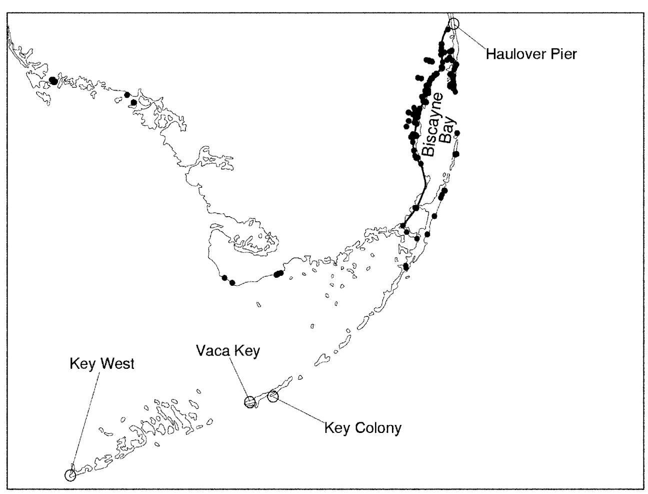

Figure 4. Locations of high water marks (solid dots) and tide gauges (circles) along the South Florida coast.

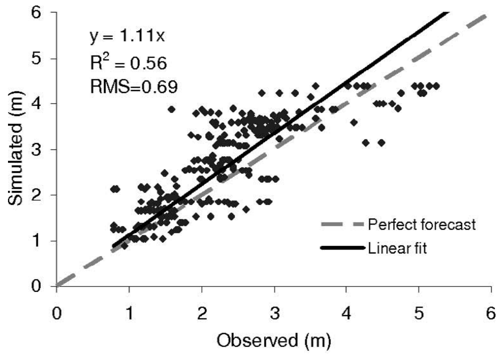

(a)

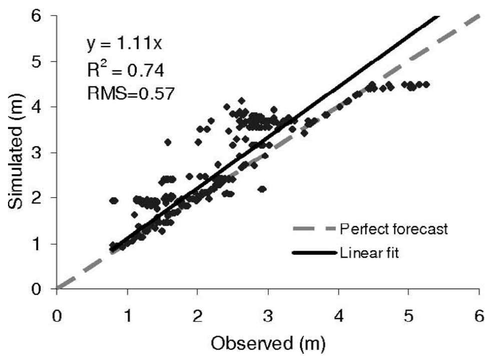

(b)

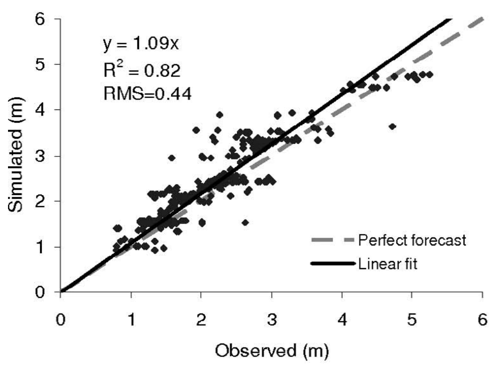

(c)

Figure 5. Comparison of observed elevations of high water marks for Hurricane Andrew with computed maximum storm surges around the Biscayne Bay coast from SLOSH (a), CEST with the coarse-resolution grid (b), and CEST with the fine-resolution grid (c). Both computed and observed maximum storm surge heights were referred to the NGVD 29 vertical datum.

The wind and atmospheric pressure model implemented in SLOSH is a parameter model from Myers and Malkin (1961). The wind and atmospheric pressure fields are generated on the basis of the parameters of atmospheric pressure drop and radius of maximum wind speed. The pressure, wind speed, and wind direction are computed from a stationary, circularly symmetric storm with the balance of forces along and normal to a surface wind trajectory. To account for the terrain effect on the wind field, two different drag coefficients were used to compute the wind field on the terrain and on the ocean, which are referred to as lake wind and ocean wind, respectively. In this way, the inland wind field can be modeled more appropriately and thus provide a better surge simulation.

When a storm surge floods low-lying areas, it often forms a thin layer of water over land. The wind stress acting on the thin sheet flow is treated differently from those on the ocean surface in the SLOSH model. The extinction coefficient ($=H$ if $0 < H < 0.3$ m or $=1$ if $H \geq 0.3$ m) is applied to the wind stress to reduce its effect on the thin layer of water.

The influence of vegetation on the wind field was also considered in the SLOSH model. Half of the average vegetation height instead of 0.3 m is used to determine the extinction coefficient for densely vegetated areas.

To maintain model comparison consistency, the wind model for SLOSH is also used to drive the CEST model in this study, although the CEST model can accept the HRD wind field and other wind model results as inputs. The wind fields for every time step were estimated by the parameter model with the use of the best track data of hurricanes.

The “best track” data for a hurricane on the basis of poststorm analysis from the National Hurricane Center (NHC) is used to estimate the atmospheric pressure and wind fields. The best track data include storm center position, maximum sustained wind, and central pressure for every 6 hours. An archive of best track data for hurricanes from 1851 to the present is available at NHC’s website (www.nhc.noaa.gov). This is the most reliable data for simulating storm surges for past events.

FIELD OBSERVATION DATA

Three types of field data are observed for storm surges. The first is water level records from tide gauges, which are the most accurate data source for storm tide. Tide gauges not only record the maximum water level, but also a time series of rising and falling water levels caused by storms and tides. Unfortunately, the distribution of tide gauges is sparse, and most of them are located along the coastline. Therefore, an accurate spatial pattern of overland surge flooding cannot be extracted from tide gauge records. Also, the failure of tide gauges often occurs when storm surges and waves are large, making the water level records incomplete.

The second type of field observations are the elevations of high water marks left on objects such as buildings and trees by storm tide floods. Among them, high water marks at the inside of a building are the most reliable because the building serves as a “stilling well” which filters out wave fluctuations. The elevations of high water marks can vary up to several

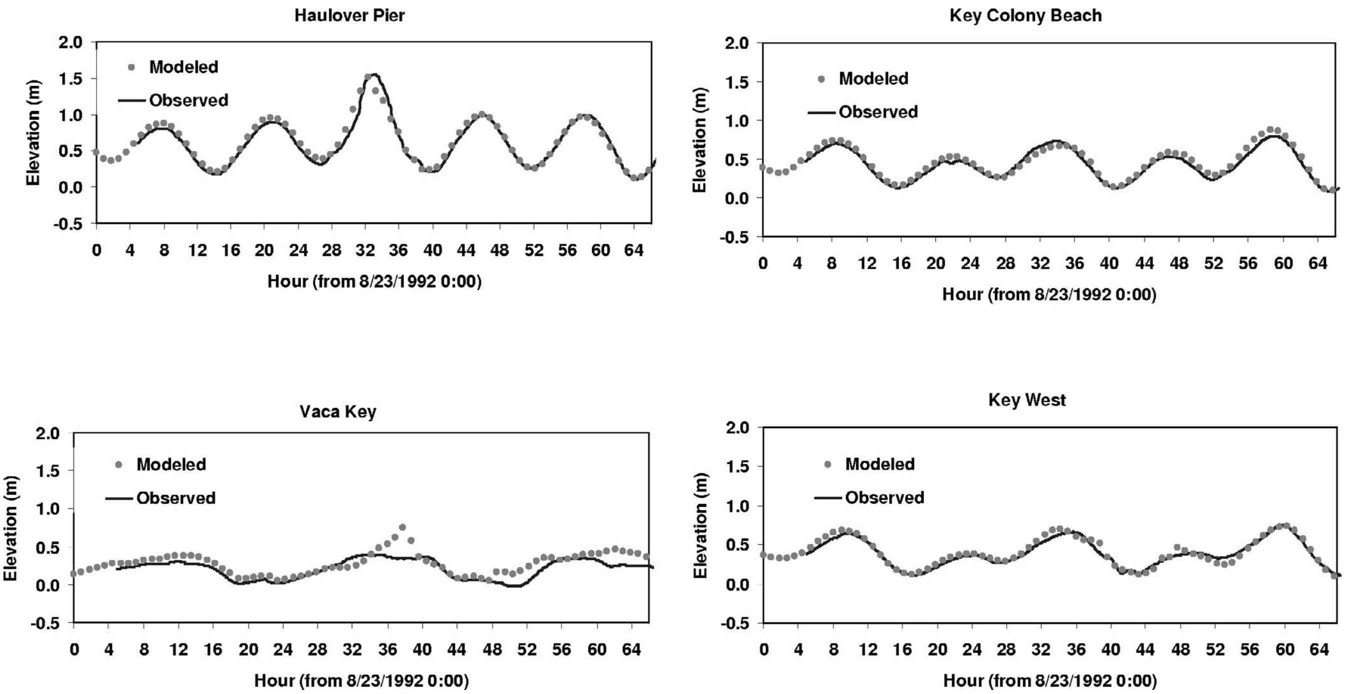

Figure 6. Modeled and field-observed time series of water levels at four tide gauges for Hurricane Andrew.

meters within a distance of several kilometers because there are so many local factors that can influence the storm tide at a specific location. However, the large-scale spatial pattern of storm tide heights can often be identified by the trend in the high water mark data (Harris, 1963).

The third type of field data is the landward inundation extent from the measurement of debris lines left by a storm. Usually, only horizontal coordinates of debris lines are recorded. The essential features of storm surge flooding for model verification can be established by analyzing the three types of field observations.

In the United States, most field data for storm surges were collected by the Federal Emergency Management Agency, USACE, USGS, and NOAA. They were usually presented in various reports by tables, figures, and maps, and only a few for recent storms are available in digital format. Comparing the model results with these data in different formats and coordinate systems is extremely inconvenient and inefficient. Geographic Information Systems (GIS) provide powerful tools to perform spatial comparison between field observations and model results. To do so, the field-observed data have to be in a georeferenced digital format. Therefore, high water marks and debris lines from different maps were digitized with commercial remote sensing software ERDAS (www.leica-geosystems.com) and ArcGIS (www.esri.com) according to the following procedure.

First, paper maps for high water marks and debris lines were scanned into the computer with an IDEAL FSC 8010 Drum Color Scanner. Second, the scanned images were registered to georeferenced digital maps. The high water marks and debris lines are usually displayed on the USGS 7.5-minute topographic quad maps with a scale of 1 : 24,000 in UTM coordinates. The georeferenced digital USGS topographic quad maps downloaded from USGS and various state agencies were employed to register scanned images. The control points for registration were derived by finding points such as tick marks, road corners, and small stream junctions in both scanned and georeferenced images. The root mean square errors of registration are about 2–5 m. Third, the debris lines and high water marks were digitized on the screen and converted into ArcGIS shapefiles.

COMPARISON OF MODEL SIMULATIONS

Hurricanes Camille of 1969, Hugo of 1989, and Andrew of 1992 were used to examine the storm surge simulation. We selected these hurricanes because (1) they are major hurricanes causing severe storm surge flooding; (2) field observations including tide gauge records, high water marks, and debris lines are relatively rich for these hurricanes; and (3) the landfall locations of these hurricanes are diversified along the U.S. East and Gulf coasts.

Hurricane Andrew

Both the SLOSH and CEST simulations were conducted over the coarse grid for 3 days. The simulated water levels consist of storm surges only because the tide component was not included in both models. Figures 2a and 2b show that the patterns of the maximum surge contours for SLOSH and CEST are similar in Biscayne Bay. Both models predicted the flood extent well at the northern mainland coast of Biscayne Bay because storm surges were blocked by the Atlantic Coastal Ridge (Figure 3). The Atlantic Coastal Ridge, orient-

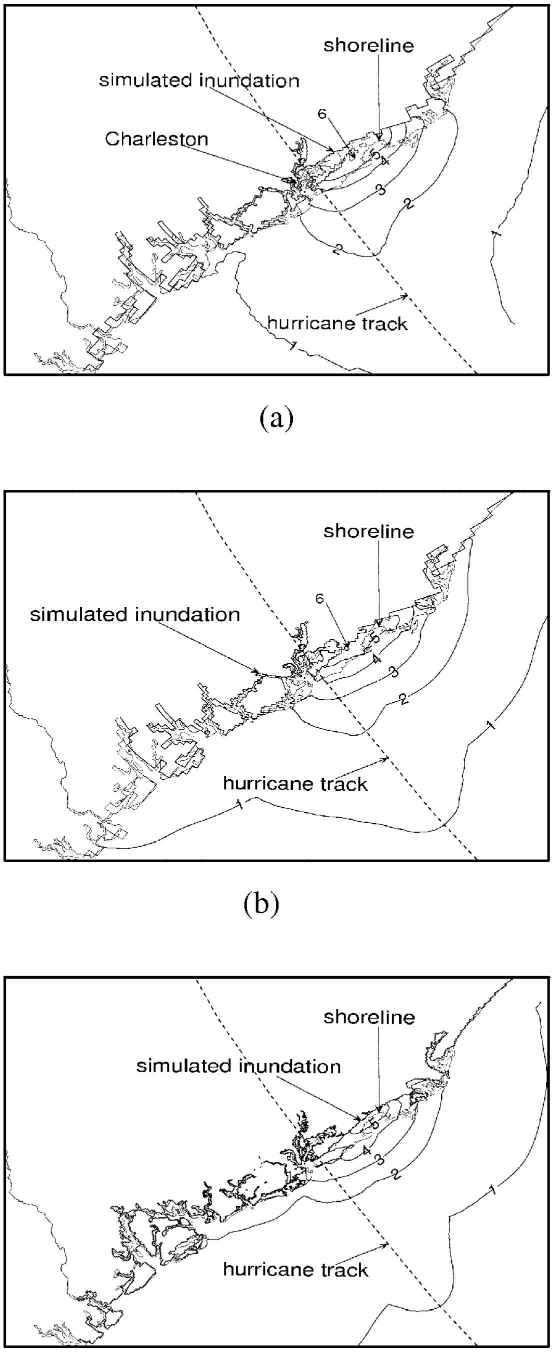

(c)

Figure 7. Contours of computed maximum storm surges and inundation lines from SLOSH (a), CEST with the coarse-resolution grid (b), and CEST with the fine-resolution grid (c) for Hurricane Hugo at the South Carolina coast.

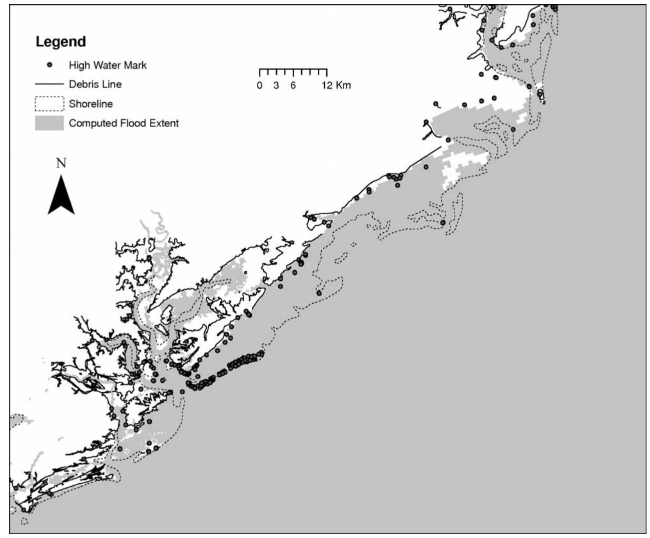

Figure 8. Comparison of simulated inundation for Hurricane Hugo by the fine-resolution CEST model with field observations.

ed north–northeast along the mainland, is 5–6 m above sea level and 8–10 km wide (HOFFMEISTER, 1974). The Ridge is close to the shore in northern Biscayne Bay and deviates away from the shore and becomes lower toward the south. Compared with the field observations (the debris line in Figure 3), the CEST model slightly underpredicted the flooding at the southern coast of Biscayne Bay, whereas the SLOSH model overpredicted the flooding considerably. This occurs because the wetting-drying algorithms for the two models are different. Also, the model grid resolution is too coarse at the south to resolve topographic features of the low-lying area at the front of the Atlantic Coastal Ridge.

Simulated maximum storm surges were compared with observed elevations of high water marks to examine the accuracy of the model results. The elevations of high water marks include the contribution from both storm surge and astronomical tide. However, storm surge is the dominant component of storm tide in south Florida because the tide range is less than 1 m. Therefore, storm surges can be compared with high water elevations directly for estimating the accuracy of simulation. High water marks were surveyed at more than 300 locations in south Florida for Hurricane Andrew (Figure 4). The simulated maximum storm surges corresponding to observed high water marks were extracted on the basis of the horizontal coordinates. A scatterplot of observations against computed values shows that the CEST model simulated maximum storm surges better than the SLOSH model with R^2 values of 0.74 compared with 0.56 (Figure 5a and 5b).

The root mean square (RMS) difference between computed and observed maximum high water levels provides another means to quantify the simulation errors. The RMS errors of computed maximum storm tides is defined as

$$e_{\mathrm{RMS}} = \sqrt{\frac{\sum_{i=1}^{n} (z_{\mathrm{c}} - z_{\mathrm{m}})^2}{n}} \quad (3)$$

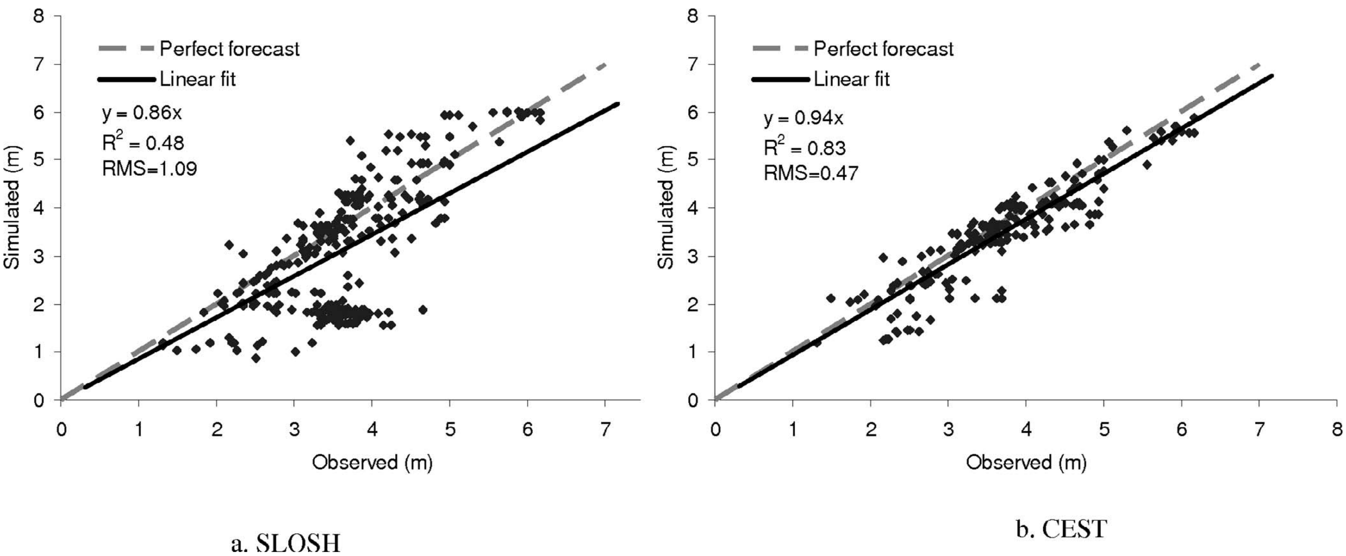

Figure 9. Comparison of observed elevations of high water marks for Hurricane Hugo with computed maximum storm tides along the South Carolina coast for SLOSH (a) and CEST (b), respectively. The SLOSH simulation was conducted over a coarse polar grid, whereas the CEST simulation was carried out over a fine-resolution curvilinear grid.

where n is the total number of high water marks, z_m is the measured elevations of high marks, and z_c is the computed maximum storm tide heights, which are set to be equal to the storm surge heights in this case. The RMS errors for computed maximum high surges are 0.57 and 0.69 for CEST and SLOSH, respectively. The better results from CEST indicate that the model improves the overland flooding prediction.

The fine-resolution curvilinear grid was used for the CEST model to simulate the storm surge with tide. The model results were obtained within 20–30 minutes on a workstation with a 2.4-GHz Pentium 4 processor and 3 gigabytes (GB) of RAM. The maximum storm tide predicted by the CEST model is presented in Figure 2c. The peak storm tide simulated by the model is about 5 m. The influence of grid resolution on abnormal high water level is more apparent when comparing the results from fine and coarse grids. Higher storm tide from the fine grid model occurs at the bay side of the barrier island south of the Biscayne Bay entrance because of strong offshore winds from the left side of the hurricane track. It appears that the storm tide looks more realistic there when the grid resolution is fine enough to resolve the barrier islands and inlets. Therefore, correctly representing these narrow barrier islands is essential to accurately simulate surge inside the Bay.

Figure 3 shows the inundation extents from the CEST model and field observations, indicating a much improved prediction of overland flooding range in contrast to the result from SLOSH (Figure 2a). Comparing storm tide predictions with observed elevations of high water marks along the coast also indicates a better prediction of flood amplitude (Figure 5c). The RMS errors of predicted maximum storm tide heights were reduced to 0.44 m. Therefore, a fine-resolution grid that represents topographic and bathymetric features better is important for improving the prediction of overland surge flooding.

Tidal gauge records provide a valuable source to examine the time process of storm tides. Unfortunately, a tide gauge record was not available at Biscayne Bay during Hurricane Andrew. However, several tide gauges were present at the edges of the north and south portions of the coastal area influenced by Hurricane Andrew (Figure 4). Comparison shows that the simulated storm tides from the fine-resolution CEST model agree well with observations at Haulover Pier, with about 1 m of storm surge; Key Colony Beach; and Key West (Figure 6). The simulated storm tides are slightly higher than observations at Vaca Key.

Hurricane Hugo

The simulation of Hugo without tide was initially conducted over a coarse polar grid. Figures 7a and 7b present the simulated maximum surge contours for SLOSH and CEST, respectively. The results show that maximum storm surges and inundation areas predicted by SLOSH and CEST are almost identical. The predicted maximum surge is approximately 6.0 m about 40 km northeast of Charleston, which agrees with the observations. The extent of the flood along the banks of creeks at estuaries were not well simulated because the coarse polar grid did not represent the convoluted shapes of these creeks.

To examine the effect of the model grid, a simulation of Hugo with CEST was conducted over a high-resolution grid. The maximum storm tides predicted by the CEST model are presented in Figure 7c. Comparison of the results of SLOSH and CEST for the fine grid indicates that predictions of maximum storm tides north of Charleston are very similar. How-

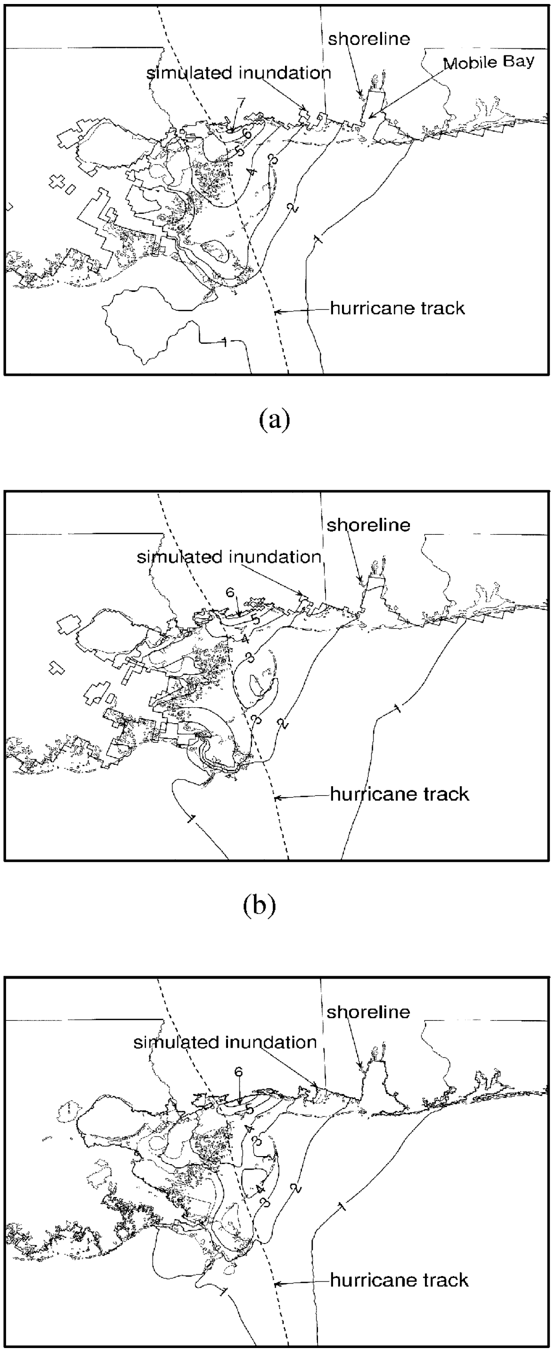

Figure 10. Contours of computed maximum storm surges and inundation lines from SLOSH (a), CEST with the coarse-resolution grid (b), and CEST with the fine-resolution grid (c) for Hurricane Camille at the Mississippi and Louisiana coasts.

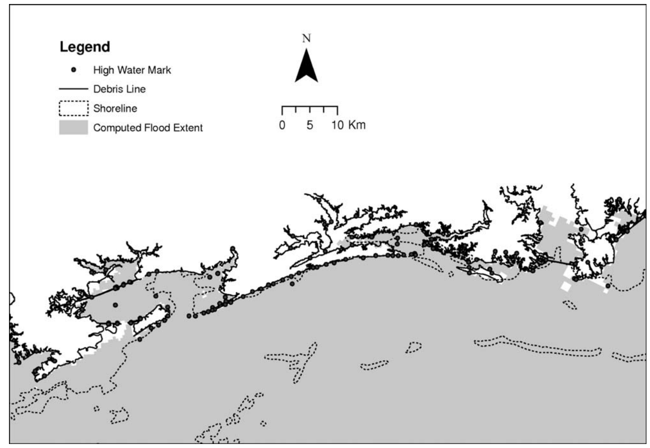

Figure 11. Comparison of simulated inundation for Hurricane Camille by the fine-resolution CEST model with field observations.

ever, the high-resolution model generated higher storm tides at the southern part of the modeling area, as indicated by the 2-m maximum storm tide contour. Figure 8 shows that the CEST simulation for the high-resolution grid agrees better with the field observations of inundation along the coastal barrier islands, indicating an improvement in flood extent prediction. The inundation simulation along the banks of creeks was also improved, but there is still considerable discrepancy between the simulated values and field observations. This probably occurs because the shapes of creeks are not well described by the bathymetric and topographic data from NOAA and USGS.

Figures 9a and 9b show scatterplots of the SLOSH and fine-resolution CEST model results compared with the elevations of high water marks. The corresponding R^2 values for SLOSH and CEST are 0.48 and 0.83, respectively. The SLOSH model produced a more scattered prediction. The points from CEST are less scattered, but the model slightly underpredicted the storm tides. The RMS errors of the SLOSH and CEST models are 1.09 and 0.47 m, respectively, indicating a better prediction from CEST.

Hurricane Camille

Both SLOSH and CEST models were tested with the coarse grid for Hurricane Camille. The meteorological data for Hurricane Camille are not well defined; the reported parameter values were used to estimate the wind field (Jelesnianski, Chen, and Shaffer, 1992). The model simulation was conducted for more than 3 days. The contours of maximum surge are shown in Figures 10a and 10b for SLOSH and CEST, respectively. Both models generated maximum surges at the right side of the hurricane track. The highest surge from the SLOSH model reached about 7.4 m, and those from the CEST model are slightly lower and reached about 7 m. The spatial pattern of computed maximum storm surges by SLOSH and CEST are similar, and both models simulated the surge well in Lake Pontchartrain.

A high-resolution grid for CEST was employed to simulate

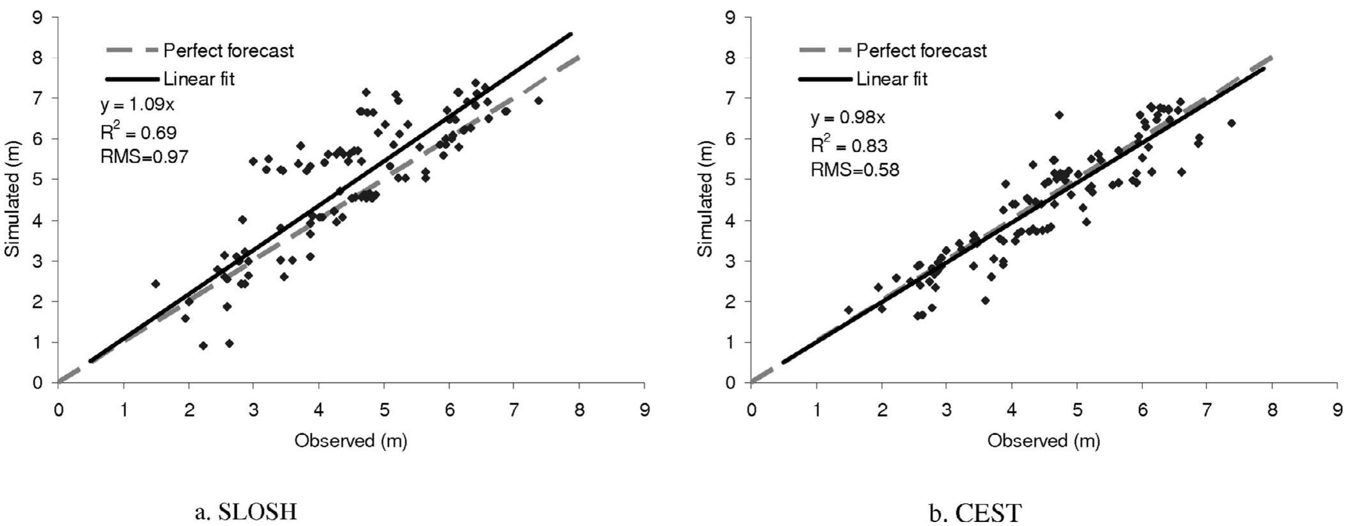

Figure 12. Comparison of observed elevations of high water marks for Hurricane Camille with computed maximum storm tides along the Mississippi and Louisiana coasts for SLOSH (a) and CEST (b). The SLOSH simulation was conducted over a coarse polar grid, whereas the CEST simulation was carried out over a fine-resolution curvilinear grid.

the Camille-induced storm tide in detail. Overall, the spatial pattern of maximum storm tides (Figure 10c) is similar to those from the coarse grid. A comparison of computed inundation lines with field-measured debris lines indicates that the CEST model, in general, simulates the inundation extent well (Figure 11). However, the simulated storm tides were not able to propagate further inland along some rivers behind the lagoons. The reason for this phenomenon is probably the result of poor delineation of river channels by the low-resolution bathymetric and topographic data.

Figures 12a and 12b show scatterplots of model results against observed high water marks along the coast for SLOSH and CEST, respectively. The corresponding R^2 values are 0.69 and 0.83, respectively. Because the inundation areas further inland were not simulated, only the areas in which the two models predicted flooding are used for comparison. It appears that CEST has a better performance on the basis of RMS errors, whereas the SLOSH model overpredicted high storm surges at the landfall area slightly.

DISCUSSION AND CONCLUSIONS

Comparison of model results from SLOSH and CEST with field observations for Hurricanes Camille, Hugo, and Andrew indicates that CEST has a better performance in predicting the magnitudes and extent of storm surge flooding. This improvement is mainly due to a better representation of important small topographic features, such as coastal ridges and barrier islands, by the fine-resolution grid and the new algorithm for wetting and drying processes. The simulations from SLOSH can also be improved if a fine–resolution model grid is utilized. However, an increase in grid resolution will multiply the computation time because a small time step is required to ensure the numerical stability of the explicit scheme used by SLOSH according to the Courant-Friedrichs-Lewy condition. For example, it takes SLOSH 42 seconds to run the 60-hour surge simulation for Hurricane Andrew with the original SLOSH grid, whereas it only takes 8 seconds for CEST to run the same-length simulation. If the grid resolution is doubled by dividing an original cell into four smaller pieces, it takes 46 minutes for SLOSH and 30 seconds for CEST to run the same simulation, respectively. All these simulations were performed on a DELL Pentium 4 workstation with a 3-GHz Xeon processor and 3 GB of RAM.

The inclusion of nonlinear items in the model equations can also cause the difference in surge simulation. To examine the effect of nonlinear items, numerical experiments with and without these items were conducted for a hypothetical hurricane landfall at Miami. The meteorological parameters for the hypothetical hurricane come from Hurricane Rita in 2005. The simulation results show that maximum surges without nonlinear terms are about a foot higher than those with nonlinear terms. Therefore, it is better not to neglect the nonlinear terms in the control equations. In addition, increase in computation time by including nonlinear items into the model has become less of concern in recent years because of a rapid growth in computation power.

The CEST model can be used to delineate evacuation zones and quantify the spatial pattern of storm surge flooding immediately after the storm when field observations are not available. The flooding information will help emergency managers respond to the storm and dispatch resources effectively. This model is also very useful for performing optimal urban planning, establishing building setbacks, and mitigating flood damage by simulating possible storm surges. The model can also simulate the tide, surge, and their interaction simultaneously, which is very useful to quantify the coastal erosion induced by storms.

Although the current algorithm improves the overland flooding computation considerably, further research is needed to make the prediction better. The overland flooding processes are not only influenced by topography, but also by the distribution of vegetation and buildings. Airborne light detection and ranging measurements (LIDAR) can provide quantitative information about heights and density of vegetation and buildings. However, little is known about interactions between surges and vegetation and buildings because field observations are lacking. Simple instruments that can be deployed quickly and extensively during a hurricane need to be developed to record the flooding processes over the land. The application of remote sensing technology such as synthetic aperture radar (SAR) imaging, which can penetrate cloud cover and detect overland flooding, also needs to be investigated.

ACKNOWLEDGMENTS

We thank Dr Jye Chen for sharing his expertise in storm surge modeling and his valuable suggestions.

LITERATURE CITED

Blumberg, A.F. and Mellor, G.L., 1987. A description of three-dimensional coastal ocean circulation model. *In:* Heaps, N.S. (ed.), *Three-Dimensional Coastal Ocean Models.* Washington, DC: American Geophysical Union, pp. 1–16.

Casulli, V. and Cheng, R.T., 1992. Semi-implicit finite difference method for three-dimensional shallow water flow. *International Journal for Numerical Methods in Fluids,* 15, 629–648.

Harris, L., 1963. *Characteristics of the Hurricane Storm Surge.* Washington, DC: Weather Bureau, U.S. Department of Commerce, 139p.

Hoffmeister, J.E., 1974. *Land from the Sea.* Miami, Florida: University of Miami Press, 143p.

Holland, G.J., 1980. An analytic model of the wind and pressure profiles in hurricanes. *Monthly Weather Review,* 108, 1212–1218.

Houston, S.H.; Shaffer, W.A.; Powell, M.D., and Chen, J., 1999. Comparisons of HRD and SLOSH surface wind fields in hurricanes: implications for storm surge and wave modeling. *Weather and Forecasting,* 14, 671–686.

Hubbert, G.D. and McInnes, K.L., 1999. A storm surge inundation model for coastal planning and impact studies. *Journal of Coastal Research,* 15, 168–185.

Jelesnianski, C.P., 1970. Bottom stress time-history in linearized equations of motion for storm surge. *Monthly Weather Review,* 98, 462–478.

Jelesnianski, C.P.; Chen, J., and Shaffer, W.A., 1992. SLOSH: Sea, Lake and Overland Surges from Hurricanes. Washington, DC: National Oceanic and Atmospheric Administration.

Kim, S.C. and Chen, J., 1999. Bottom stress of wind-driven currents over an inner shelf determined from depth-integrated storm surge model. *Journal of Coastal Research,* 15(3), 766–773.

Mukai, A.Y.; Westerink, J.J.; Luettich, R.A., and Mark, D., 2002. Eastcoast 2001, A Tidal Constituent Database for Western North Atlantic, Gulf of Mexico, and Caribbean Sea. Vicksburg, Mississippi: U.S. Army Corps of Engineers, 23p.

Myers, V.A. and Malkin, W., 1961. Some Properties of Hurricane Wind Fields as Deduced from Trajectories. Washington, DC: NOAA, 43p.

Powell, M.D.; Houston, S.H.; Amat, L.R., and Morisseau-Leroy, N., 1998. The HRD real-time hurricane wind analysis program. *Journal of Wind Engineering and Industrial Aerodynamics,* 77/78, 53–64.

Scheffner, N.W. and Fitzpatrick, P.L., 1997. Real-time predictions of surge propagation. *In:* Malcolm, L. and Spaulding, M.L. (eds.), *Estuarine and Coastal Modeling.* Alexandria, Virginia: ASCE, pp. 374–388.

Shi, F.; Sun, W., and Wei, G., 1997. A WDM method on generalized curvilinear grid for calculation of storm surge flooding. *Applied Ocean Research,* 19, 275–282.

Tang, Y.M. and Grimshaw, R., 1995. A model analysis of coastally trapped waves generated by tropical cyclones. *Journal of Physical Oceanography,* 25, 1577–1598.

Xiao, C.; Zhang, K., and Shen, J., 2006. CEST: A Three-Dimensional Coastal and Estuarine Storm Tide Model. Miami, Florida: International Hurricane Research Center, Florida International University, 20p.